Photoionization Studies of Chromophore-Labeled Amino Acids and Peptides†

Christopher T. Houston and James P. Reilly*

Department of Chemistry, Indiana University, Bloomington, Indiana 47405

Received: March 31, 2000; In Final Form: June 26, 2000

The photoionization characteristics of a naphthol chromophore covalently tethered to a few different amino acids and small peptides are investigated. To isolate the chromophore from the biological molecules the linkage between them is constructed from saturated alkyl chains of up to 12 carbons in length. Experimental results are compared with those of previous studies that explored the photoionization of macromolecules.

Introduction

For over two decades, multiphoton ionization experiments have facilitated the extraction of spectroscopic information about the excited states of small molecules[1−3] and the vibrational levels of ions.[4−7] In the earliest studies in this field, gas cells with electrodes were used to record the wavelength dependence of molecular ionization yields. However, it was soon apparent that mass spectrometers were better suited for both detecting and identifying ions. Time-of-flight mass spectrometers became particularly popular because of their simplicity of construction and ability to resolve all ions produced by each laser pulse.[8−11] Following the success of these multiphoton ionization mass spectroscopic investigations on small molecules, the prospect of performing similar studies on biological systems seemed attractive. Unfortunately, macromolecules irradiated with appropriately energetic light exhibit little tendency to ionize.[12−14] This is noteworthy considering that an alternative method, matrix-assisted laser desorption/ionization (MALDI), has been very successful at generating singly charged intact gas-phase macromolecular ions.[15,16] The key difference between these experiments is that while photoionization involves the ejection of an electron from a neutral molecule, the MALDI phenomenon involves the desorption of matrix-entrained macromolecules into the gas phase and the ionization of some fraction of these molecules by proton or cation transfer reactions. Although it is commonly believed that this ionized fraction is small,[17] parent ion yields are sufficient to produce high quality mass spectra of proteins, nucleic acids, carbohydrates, and even synthetic polymers. Nevertheless, the putative abundance of intact neutral molecules makes a MALDI desorption plume an attractive photoionization target. If these neutral molecules could be efficiently ionized, a number of advantages might accrue. First, there would be a potential gain in sensitivity. Second, because photoionization is a physical process, its efficiency might be more consistent and predictable than that of MALDI. Third, gas-phase photoionization should produce sharp mass spectral peak shapes. The resolving power of TOF mass analyzers is limited by the temporal characteristics of the ionization source and the initial spatial and energy distributions possessed by the nascent ions.[18,19] A well-focused, short-pulse-duration photoionization laser that only samples neutrals having similar kinetic energies should lead to excellent results. This prospect provided part of the motivation behind this work.

In the familiar photoelectric effect, electrons are ejected from metal surfaces. It therefore may not seem surprising that large metal clusters photoionize with facility.[20,21] In contrast, as alluded to above, ionization studies on organic and biological molecules have generally been rather discouraging. The limited successes that have been achieved can be easily enumerated. Frey and Holle photoionized gramicidin D (MW = 1881 Da) using infrared laser desorption followed by jet cooling and resonant laser ionization at 270 nm.[22] Schlag et al. demonstrated that photoionization yields drop monotonically as the size of molecules increases and cited previous evidence of a measurable delay between excitation of large molecules and release of photoelectrons.[12,13] Subsequently, they demonstrated that parent ion yields for gramicidin S (MW = 1141 Da) and gramicidin D are higher with femtosecond than with nanosecond duration light pulses.[14] They argued that, as atoms are added to a molecule, energy imparted to the system may be dissipated into a growing number of vibrational modes before ionization can occur.[12] Becker and Wu successfully photoionized gramicidin S with nontunable vacuum UV, but could not form intact parent ions for substance P (MW = 1348 Da) or gramicidin D.[23] They proposed that fragmentation of the peptide dominates over ionization in most cases. Reilly and Reilly demonstrated that the laser desorption and multiphoton ionization of tryptophan leads to fragment ions unless the desorption is conducted in such a way that some molecular cooling is induced.[24]

Some authors have coupled a near-UV absorbing chromophore to biological molecules. Li and Lubman studied several CBZ-labeled nonaromatic peptides.[25] Neutral molecules were laser desorbed and entrained in a jet expansion using a method introduced by Weyssenhoff et al.[26] They successfully two-photon ionized a tri-peptide but noted that their sensitivity decreased with peptide size. Levis and co-workers two-photon ionized a single deoxythymine monophosphate with a covalently attached anthracene chromophore, but they did not present data for the photoionization of any larger biological molecules.[27] Anex et al. two-photon ionized a jet-cooled perfluorinated polyether with a terminal phenol present as a chromophore using 193 nm ArF laser light.[28] Remarkably, they observed polymer ions with masses up to 7000 Da. The one characteristic that all of the successful laser ionization experiments share is that sample molecules were supersonically cooled. Even so, the perfluorinated polyether experiment stands out as unique; without jet cooling, molecules having masses of 1 to 2 kDa generally do not ionize.

† Part of the special issue "C. Bradley Moore Festschrift".

* Corresponding author.

10.1021/jp001246t CCC: $19.00
Published on Web 08/10/2000

Difficulties associated with ionizing nonjet-cooled macromolecules have been attributed to the molecule acting as a solvent for the excited electron; the ion−electron complex may effectively relax to isoenergetic vibronic levels whose density increases with molecular size.[12−14] The fact that some jet-cooled macromolecules have been successfully photoionized (by one- or two-photon processes) has led to the suggestion that macromolecules actually do photoionize but they subsequently fragment, preventing parent ions from being detected.[23] Evidence of fragment ion production, which would support this contention, is sought in the current experiments. In any case, the contrasting ionizing propensities of metallic clusters compared to organic and biomolecules have never been explained. The electronic transition moment associated with the photoionization process can be written:[29]

$$M_e(r;R_0) = \int \psi_e^{*\prime}(r;R_0)\,|\sum_i p_e|\,\psi_e'(r;R_0)\mathrm{d}r \qquad (1)$$

Here r refers to electron coordinates and R_0 to nuclear coordinates (that are assumed to be fixed at the equilibrium ground state configuration). Inspection of this integral suggests yet another possible explanation for the low photoionization yields of macromolecules. To the extent that the ground and excited wave functions can be written as properly antisymmetrized products of the form

$$\psi_e = \phi_1(r_1;R_0)\,\phi_2(r_2;R_0)\,\phi_3(r_3;R_0)\,...\,\phi_n(r_n;R_0) \qquad (2)$$

then the transition moment will involve the sum of integral products. The number of integrals in each of these products corresponds to the number of electrons in the molecule. For macromolecules with thousands of electrons, thousands of overlap integrals contribute to each term in the sum. If each of these were slightly less than unity because of small shifts in the distribution of electrons during the ionization process then the product of thousands of such integrals would be a small number, leading to a small photoionization transition moment. To the extent that this effect contributes to the low ionization yields, the covalent attachment of a photoionization chromophore to a macromolecule might be expected to improve the ionization yield, *as long as the chromophore is sufficiently isolated from the rest of the molecule that the electrons of the macromolecule are unaffected by the electronic transition in the chromophore*. In the present work, we investigate the photoionizing characteristics of naphthol both as an isolated gas-phase molecule and when bonded through a 6- or 12-carbon alkyl chain to a few amino acids and peptides. This paper describes our efforts to produce photoionized biological molecules derivatized to such a chromophore.

Experimental Section

Materials. The synthesis reagents acetyl chloride, benzyl chloroformate, 12-bromododecanoic acid, 6-bromohexanoic acid, camphorsulfonic acid, *N*,*N*-dimethylformamide, 4-(dimethylamino)pyridine, ethylchloroformate, 2-naphthol, and triethylamine were obtained from Aldrich (Milwaukee, WI). Valine, leucine, trialanine, and bradykinin and the MALDI matrix compound α-cyano-4-hydroxycinnamic acid were purchased from Sigma (St. Louis, MO).

Synthesis of 12-(2-Naphthoxy)dodecanoic Acid (NDA). 12-Bromododecanoic acid was protected during the synthesis by conversion to the ethyl ester. An amount of 0.524 g (1.88 mmol) of the acid was added to 2 mL ethanol (34.3 mmol) in the presence of camphorsulfonic acid as catalyst. The mixture was boiled under reflux overnight. Next, 0.38 g (2.63 mmol) of 2-naphthol were combined with 2.35 mmol of sodium hydride in 5 mL of tetrahydrofuran (THF). Sodium hydride was added as a 60% suspension in oil. An amount of 0.4 g (1.30 mmol) of bromododecanoic acid ethyl ester was added to the mixture and boiled under reflux overnight. Preparative-scale silica column chromatography in 5:1 hexanes/ethyl acetate was employed to purify NDA−ethyl ester from starting reagents. NDA was generated by dissolution of the ester in 5 mL of THF and 4 mL of 1 M NaOH (aq). The solution was stirred 48 h. Addition of CH_2Cl_2 precipitated NDA as the sodium salt. Three washes in CH_2Cl_2 removed much of the contaminating ethyl ester. Next, 1 M HCl (aq) was added to the aqueous mixture and NDA was extracted into CH_2Cl_2 and dried over sodium sulfate. Product identity was verified by ^{1}H NMR and laser desorption/photoionization mass spectrometry.

Synthesis of 6-(2-Naphthoxy)hexanoic Acid (NHA). A slightly different approach was employed to synthesize an analogous phototag compound with a six- carbon chain (NHA). The precursor acid (6-bromohexanoic acid) was protected with a benzyl ester that is easily removable by hydrogenation. This ester was prepared according to the method of Kim et al.[30] by combining 2 g (10.25 mmol) of bromohexanoic acid with 1.46 mL (10.253 mmol) of benzylchloroformate and 1.9 mL of triethylamine (13.33 mmol) in the presence of a catalytic amount of 4-(dimethylamino)pyridine. These reagents were stirred under nitrogen for 1 h in CH_2Cl_2.

Formation of NHA−benzyl ester was accomplished by the method of Allen and Gates.[31] An amount of 0.609 g (2.128 mmol) of bromohexanoic acid benzyl ester was combined with 0.256 g (1.773 mmol) of 2-naphthol, and 0.246 g (1.773 mmol) of potassium carbonate in acetone. This mixture was boiled under reflux for 4 days. After removal of the acetone in vacuo, the mixture was dissolved in diethyl ether and washed three times with saturated sodium carbonate followed by three washes with pH 7 phosphate buffer. The ether layer containing NHA−benzyl ester was collected, dried over magnesium sulfate, and evaporated to dryness. The crude product was subsequently purified using a preparative-scale silica column run in 5:1 hexanes/ethyl acetate. Although unreacted 2-naphthol was removed from the product, ^{1}H NMR revealed that a small amount of 6-bromohexanoic acid remained.

The final product (NHA) was generated by hydrogenation of NHA−benzyl ester. This reaction was run in ethanol under a hydrogen atmosphere in the presence of Pd-activated carbon. Contrary to our original anticipation, conversion of the ester to NHA was not quantitative, but proceeded with approximately 50% yield. A second preparative-scale silica column was therefore employed with 1:1 hexanes/ethyl acetate to separate NHA−benzyl ester from NHA. The final product contained a small amount of 6-bromohexanoic acid present as an impurity.

Activation of NDA and NHA for Reaction with Biological Molecules. NDA and NHA were converted to mixed anhydrides (**I**) to activate them for covalent attachment to a target biological molecule. This derivative was prepared by dissolving NDA or NHA in dry CH_2Cl_2 and adding 0.9 equivalents of triethylamine at 0 °C under nitrogen. An amount of 1.1 equivalents of ethylchloroformate were added dropwise to the mixture. Following an additional hour of stirring at room temperature under nitrogen, the mixture was diluted into diethyl ether to precipitate the triethylammonium chloride byproduct. This salt was removed by filtration and the resulting solution was evaporated to dryness to remove excess ethylchloroformate.

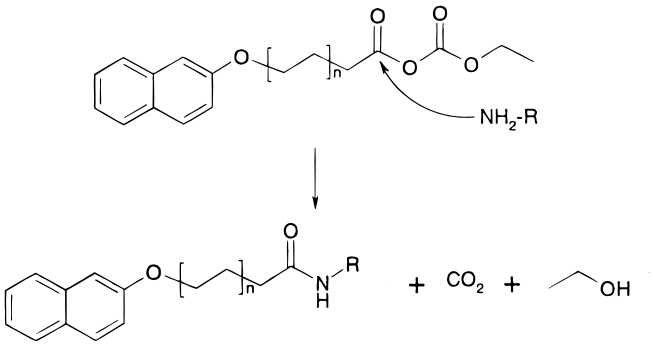

Figure 1. Reaction scheme for phototag ($n = 2$ for NHA, $n = 5$ for NDA) activated by mixed anhydride derivatization. A primary amine in the target biological molecule attacks the carbonyl, forming a new peptide bond.

Figure 1 illustrates how the mixed anhydride derivatives react with primary amines to label biological molecules.[32] These activated phototag compounds were mixed equimolar (or in slight excess) with the target biological molecule. *N*,*N*-dimethylformamide (DMF) was chosen as a solvent for this reaction as it successfully dissolves NDA, NHA, and the biological molecules studied.

Esterification of Amino Acids. The solubility of single amino acids in DMF was enhanced by converting them to methyl esters via the method reported by Kowalack and Walsh.[33] Methanolic 2 N HCl was prepared by adding 8.5 mL of anhydrous methanol to 1.5 mL of acetyl chloride. After 10 minutes of stirring at room temperature, the mixture was ready for use. Amino acids were mixed with a large excess of methanolic 2N HCl (1 mg of amino acid/100 μL of esterification reagent) in 1.5 mL Eppendorf tubes. Samples were incubated at 37 °C for 4 h. A small hole was made in the top of the sealed Eppendorf tubes to relieve the gas pressure that accumulates during the reaction. Once the reaction was complete, excess esterification reagent was removed in vacuo.

HPLC Purification of NHA−Bradykinin. NHA-derivatized bradykinin was purified using a Dionex GPM-2 HPLC system. An Alltech Hypersil ODS (C18) column was used for the separation. A linear gradient of 50%−100% ethanol in 0.1% aqueous trifluoroacetic acid was run for 60 min at 1 mL/min. Absorbance detection was performed at 286 nm, the λ_{max} of 2-naphthol.[34] Fractions were collected in 1.5 mL Eppendorf tubes. Solvent was removed in a Jouan RC1010 SpeedVac vacuum centrifuge, and the samples were reconstituted in ethanol. Fraction identity and purity were established by delayed extraction MALDI-TOF and DC photoionization experiments.

Time-of-Flight Mass Spectrometry. Mass spectrometry was performed using a linear time-of-flight instrument constructed in-house. The design of this instrument is similar to one reported previously.[35] A two-laser setup was employed to desorb and ionize phototagged biological molecules. Neutral analyte molecules were desorbed into the gas phase following cocrystallization in a MALDI matrix and irradiation at 355 nm by a frequency-tripled Nd:YAG laser (Quanta Ray DCR-2). Two-photon ionization of neutrals in the desorption plume was achieved using a XeCl excimer laser at 308 nm (Lumonics, TE-430).

The chromophore and laser system used in this study were chosen such that the incident laser radiation matched the ionization potential of the chromophore closely. Our chromophore, 2-naphthol, has an extinction coefficient of approximately 1200 M^{-1} cm^{-1} at 308 nm (measured in ethanol)[36] and an ionization potential of 7.85 eV.[37] Thus, we expect our

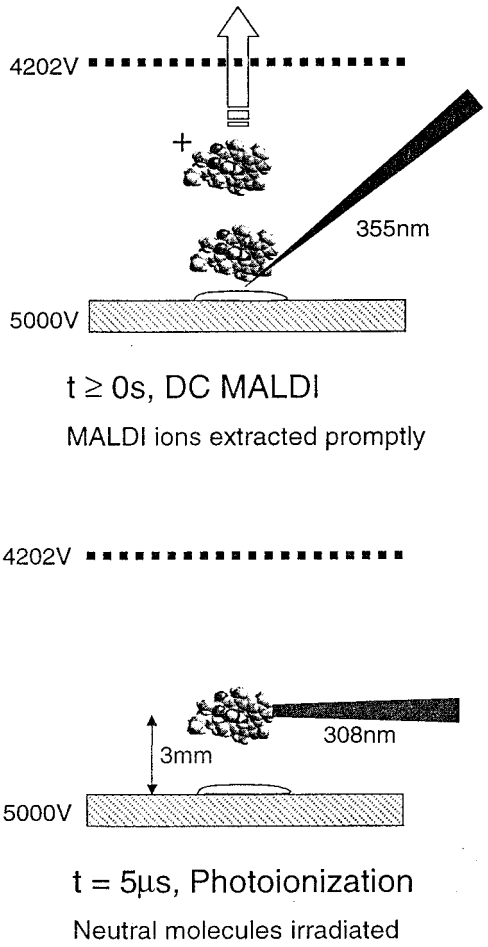

Figure 2. Experimental setup for photoionization experiments. The repeller plate and first extraction grid are held at 5000 and 4202 V, respectively. Upon desorption of analyte from the sample ($t \geq 0$ μs) by 355 nm irradiation, MALDI ions are promptly extracted while neutrals drift at their initial desorption velocity. At $t = 5$ μs, the XeCl excimer laser is fired to intersect and ionize the packet of neutrals.

phototag compounds to undergo efficient two-photon ionization from the 308 nm (4.03 eV) radiation emitted from the XeCl laser.

By design, ions were formed both by the first laser through the MALDI process and by the second laser through two-photon ionization of neutrals. To simplify data interpretation, we configured the ionization source of our mass spectrometer, displayed in Figure 2, to accelerate MALDI $[M + H]^+$ ions out of the source region prior to the photoionization step. The MALDI ions were not of interest in this experiment; matrix-assisted laser desorption was simply a convenient way to generate gas-phase neutrals. Therefore, the ionization source was set up for continuous extraction using Wiley−McLaren space-focusing.[18] Once MALDI ions were accelerated out of the ion source, an expanding plume of desorbed neutrals was left behind. Assuming an average desorption velocity of 600 m/s,[38,39] neutrals travel 3 mm in our ion source in 5.0 μs. Light from the XeCl excimer laser at 308 nm aligned parallel to and 3 mm above the sample probe was focused by a cylindrical lens such that the beam waist was immediately above the MALDI sample. This laser has a 5 ns fwhm pulse duration and was timed to fire exactly 5.0 μs after sample desorption by the Nd:YAG laser. Thus, photoions formed by XeCl laser irradiation trail MALDI-generated ions of the same mass by 5 μs, effectively decoupling ions formed from each process.

Samples were prepared by mixing 1 μL sample solution with

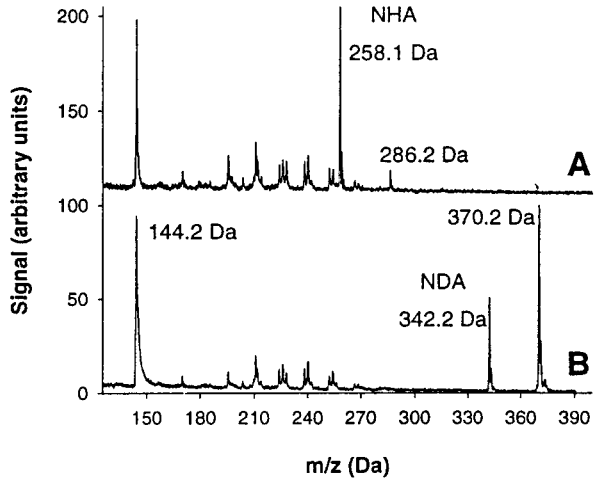

Figure 3. Photoionization mass spectra of (A) NHA and (B) NDA. The mass signals between 200 and 270 Da correspond to photoionization of pump oil background. The 286.2 and 370.2 Da peaks are ethyl ester forms of NHA and NDA, respectively.

9 μL of α-cyano-4-hydroxycinnamic acid (αCHCA) solution. An amount of 0.5 μL of the resulting mixture was deposited onto the stainless steel sample probe. αCHCA was prepared as a 10 mg/mL solution in 2:1 acetonitrile/0.1% TFA (aq). Because many MALDI samples prepared in this study contained DMF, it was necessary to warm the stainless steel MALDI probe with a heat gun to expedite drying. αCHCA MALDI spots thus prepared tend to have a smooth, glassy appearance.

Photoionization mass spectra were externally calibrated with a mixture of 2-naphthol (m/z = 144.1 Da), anthracene (m/z = 178.1 Da), and pyrene (m/z = 202.1 Da). These compounds were dissolved in DMF and deposited onto the sample probe in the matrix mixture described above. The reported molecular weights are monoisotopic values because the XeCl photoionization laser has a sufficiently short pulse duration (5 ns fwhm) to produce isotopically resolved ions under our experimental conditions. Because the acquired spectra contain contributions from photoionized and MALDI-generated ions, each spectrum can be viewed as having two separate mass scales whose origins are temporally separated by 5.0 μs, the time delay between the desorption and photoionization lasers. Given that MALDI ions are not the focus of this work, spectra are generally displayed with the photoionization mass scale. When it is useful to exhibit both MALDI and photoionization signals, spectra are plotted linear in time-of-flight relative to the firing of the photoionization laser.

All photoionization mass spectra in this paper were acquired at a 1 GHz digitizing rate and represent the summation of 100 individual laser shots unless otherwise noted. Sigma Plot version 4.1 (SPSS, Chicago, IL) was used for all nonlinear curve fitting.

Results and Discussion

Table 1 summarizes the compounds investigated in this work. Our preliminary experiments focused on photoionizing the tag compound prior to labeling any biological molecules. As shown in Figure 3, both NHA (A) and NDA (B) are easily desorbed and laser-ionized. Some additional features in these spectra are noteworthy. The cluster of ions appearing in the m/z range of 200 to 270 Da corresponds to photoionization of pump oil in the mass spectrometer. This was confirmed by acquiring similar spectra without the sample probe inserted and with the desorption laser blocked, thus eliminating the possibility that these signals could be species subliming into the vacuum from the sample or ablated by the desorption laser. Although the pressure in the ionization source during these experiments was typically (3 to 5) $\times$ 10^{-7} Torr, sufficient oil was present to give rise to these background signals. Each phototag spectrum contains a second signal 28.0 Da higher in mass than the tag itself. These compounds are ethyl ester forms of the tag molecules. Phototag molecules activated by derivatization to the mixed anhydride (**I**) are moisture sensitive and hydrolyze back to carboxylic acids

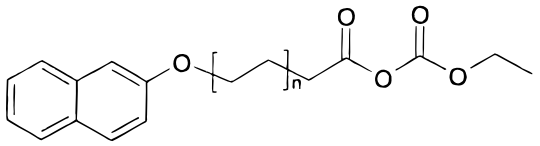

I (n = 2,5)

NHA and NDA upon exposure to water. As shown in Figure 1, ethanol is generated as a byproduct of mixed anhydride decomposition. Ethanol can attack the mixed anhydride to generate the ethyl esters. Because the activated phototags do not age well, NDA and NHA were always converted to mixed anhydrides immediately prior to reaction with a biological molecule.

A conspicuous feature in these spectra is the relatively intense, rather broad peak at m/z = 144.2 Da. This peak is indicative of a photolytic loss of the naphthol chromophore from the rest of the tag molecule accompanied by a rearrangement and is discussed later.

Our first tagging experiments used NDA-derivatized amino acids. As mentioned in the Experimental Section, each amino acid was converted to a methyl ester for improved solubility in DMF. Representative data are shown in Figure 4 for NDA-tagged valine, leucine, and trialanine. These mass spectra reveal that NDA-labeled biological molecules photoionize. It is noteworthy that, as the molecular weight of the tagged molecule

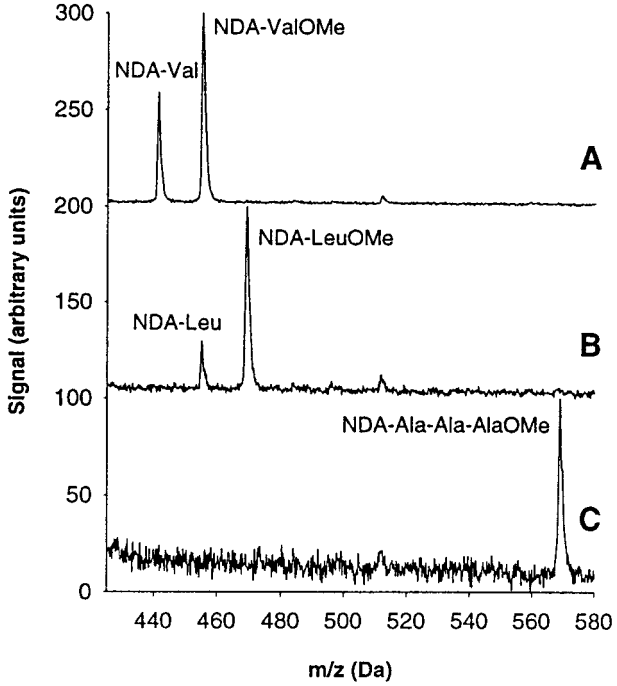

Figure 4. Photoionization spectra of amino acids tagged by NDA. Isotope-averaged masses for each peak are NDA-Val: 441.6 Da, NDA-ValOMe (OMe = methyl ester): 455.6 Da, NDA-Leu: 455.6 Da, NDA-LeuOMe: 469.6 Da, and NDA-Ala-Ala-AlaOMe: 569.7 Da.

TABLE 1: Compounds Studied by Two-Laser Desorption/Photoionization

Name	Structure
Tag Materials:	
2-naphthol	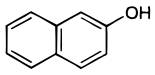
6-(2-naphthoxy)hexanoic acid (NHA)	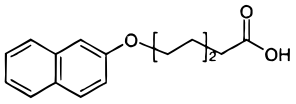
12-(2-naphthoxy)dodecanoic acid (NDA)	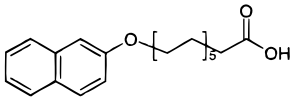
Tagged Amino Acids:	
NDA-valine methyl ester	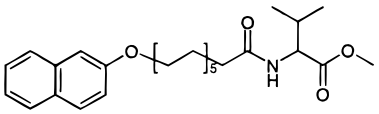
NDA-leucine ethyl ester	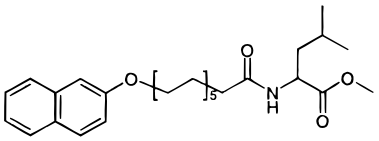
NDA-trialanine methyl ester	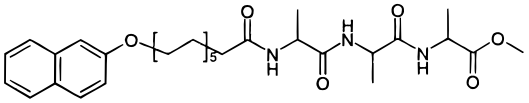
Tagged Peptides:	
NHA-bradykinin	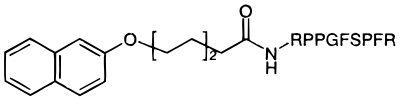
NDA-bradykinin	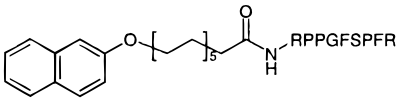

increases, photoionization becomes less efficient as evidenced by the reduction in signal-to-noise of the tripeptide (C) compared to Val (A) and Leu (B). This is, in fact, consistent with the observations made by Li, Schlag, and their co-workers.[12,25]

Although the feasibility of the tagging approach has been demonstrated, photoionization of larger biological molecules was the principal goal of this work. Subsequent experiments were conducted on the peptide bradykinin (RPPGFSPFR, MW = 1060.2 Da) derivatized with NDA and NHA. A conventional MALDI experiment with delayed extraction was employed to confirm that the expected NDA- and NHA-labeled bradykinin compounds had been successfully prepared. As demonstrated by the MALDI spectra in Figure 5, coupling NDA or NHA to this peptide resulted in a single attachment of phototag to bradykinin, very likely at the N-terminus of the peptide as no other strong nucleophiles are available. This is confirmed by the absence of peaks at $[M + H]^+ = 1710.1$ Da or $[M + H]^+ = 1541.8$ Da that would correspond to attachment of two NDA or NHA, respectively, to bradykinin. Also noteworthy is the lack of abundant side products from these reactions. The only nonnegligible side-product is the 6-bromohexanoic acid adduct in Figure 5C that results from starting material present in the final NHA product. Fortunately, this product can be readily removed from NHA−bradykinin by HPLC as evident in Figure 5D. The peaks that appear at higher mass than NHA−bradykinin in Figure 5D correspond to alkali cation adducts.

In an attempt to photoionize NDA- and NHA-labeled bradykinin, two-laser experiments were conducted. The time-of-flight mass spectrum in Figure 6 displays the results. Note that a mass scale was not applied to this spectrum because of the presence of both photoions and MALDI ions formed 5 μs apart. The time-of-flight axis is calibrated relative to the firing

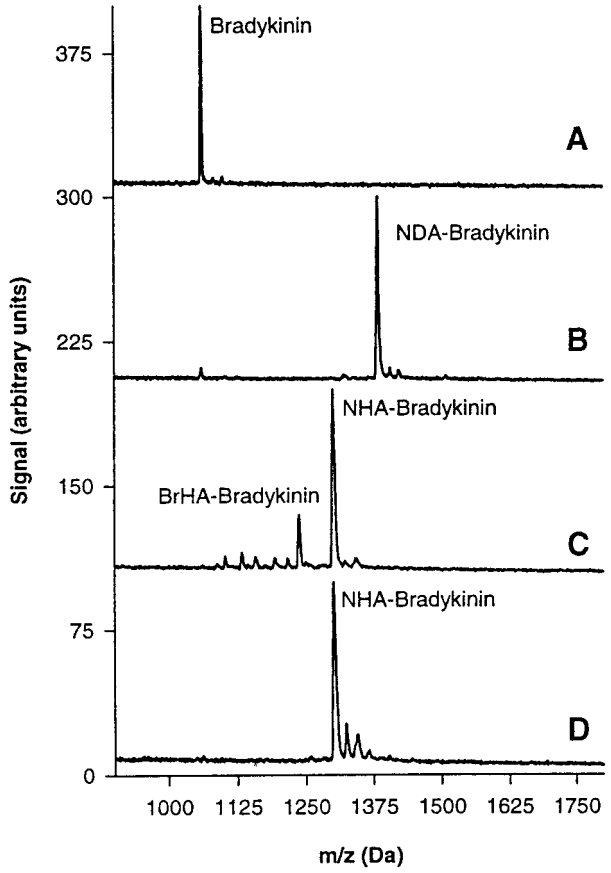

Figure 5. Delayed extraction MALDI mass spectra of (A) bradykinin ($[M + H]^+ = 1061.2$ Da), (B) NDA−bradykinin ($[M + H]^+ = 1385.7$ Da), (C) NHA−bradykinin ($[M + H]^+ = 1301.5$ Da), and (D) HPLC-purified NHA−bradykinin. NHA has a 6-bromohexanoic acid contaminant that can also label a biological molecule (BrHA−bradykinin, $[M + H]^+ = 1238.3$ Da). In (D), this contaminant has been removed by HPLC.

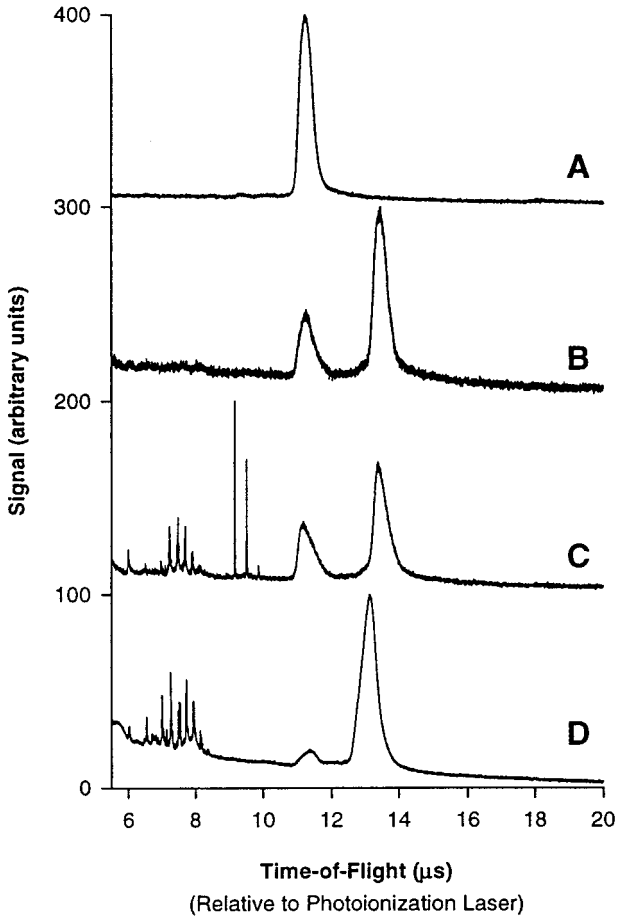

Figure 6. Continuous extraction time-of-flight mass spectra of (A) bradykinin, (B, C) NDA-labeled bradykinin, and (D) HPLC-purified NHA−bradykinin. (A) and (B) were acquired with the 355 nm desorption laser only. (C) and (D) were acquired with the 355 nm desorption and 308 nm photoionization lasers.

of the XeCl laser. Figure 6A,B displays MALDI spectra of unlabeled bradykinin and NDA-derivatized bradykinin acquired with the 308 nm photoionization beam blocked. The peak at 13.4 μs corresponds to MALDI-generated ions of NDA−bradykinin. Note some underivatized bradykinin ions appear at 11.3 μs. With the photoionization laser also passing through the ionization source, the Figure 6C spectrum of NDA−bradykinin was recorded. Photoions for unreacted NDA and NDA−ethyl ester appear as sharp signals at 9.2 and 9.6 μs, respectively. Pump oil background appears between about 6.5 and 8.0 μs. Also present is a 144 Da photofragment ion peak at approximately 6.0 μs. The NHA−bradykinin was HPLC-purified in order to eliminate unreacted phototag molecules and other side products from the mixture. Its photoionization mass spectrum is presented in Figure 6D. MALDI-formed ions corresponding to underivatized and NHA−bradykinin appear at flight times of 11.3 and 13.1 μs. Because free NHA was removed from this sample, any photoions appearing in this spectrum must correspond to species generated from NHA−bradykinin. (Unfortunately, solubility issues prevented us from purifying NDA−bradykinin in this manner). While the other spectra are averages of 100 individual laser shots, Figure 6D was recorded by averaging 1000 light pulses in order to improve its signal-to-noise ratio. Molecular photoions corresponding to NDA- or NHA-labeled bradykinin were expected to appear at flight times of 18.1 and 18.4 μs, respectively. However, the only photoion peak derived from these molecules corresponds to a fragment ion at 6.0 μs.

The most striking feature of the spectra in Figure 6 is the sharpness of photoion peaks relative to those created by MALDI. Because this linear time-of-flight instrument is configured for space focusing under continuous extraction conditions, no velocity focusing occurs. Since MALDI ions are known to have a wide velocity distribution,[38,39] broad mass spectral peaks result. With photoionization, the narrowness of the light pulse in space and time eliminates the need for velocity focusing. When the delay time between the desorption and photoionization lasers is varied from 3.0 to 7.5 μs, the photoionization mass spectrum does not change. This illustrates that the desorbed neutrals have a velocity spread of *at least* 400 to 1000 m/s. Spectral features are sharp because the laser only interrogates neutrals possessing a small range of velocities.

The lack of observed molecular photoions is consistent with the picture of Schlag and co-workers[12−14] that an increasing vibrational state density facilitates relaxation of the ion−electron complex produced by light excitation. The data in Figures 4 and 6 clearly indicate that ionization efficiency decreases as the size of the tagged biological molecule increases, regardless of the insulating alkyl chain that we interposed between the naphthalene chromophore and the biological analyte.

Becker and Wu have proposed a mechanism whereby irradiation leads to efficient photofragmentation of large molecules.[23] The weak fragment peak in Figure 6D indeed suggests that some NHA−bradykinin is photoionized and then photofragmented. However, this fragment peak is very weak. Inspecting the entire low-mass region of our data (not shown), we

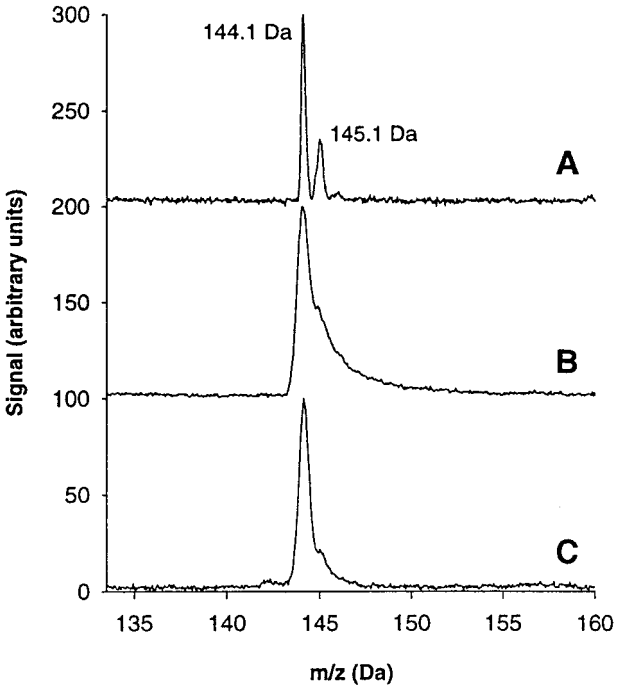

Figure 7. Photoionization mass spectra of (A) 2-naphthol, (B) the fragment ion formed from NDA, and (C) the fragment ion formed from NHA.

detected no other significant peaks that could be associated with photoionization/photofragmentation processes. We thus find very little evidence supporting the conjecture of Becker and Wu.

A closer examination of the $m/z = 144.2$ Da fragment ion peak that appears in Figure 3 conveys information about its mechanism of formation. An expanded view of this region of the spectrum is displayed in Figure 7. For comparison, the photoionization spectrum of 2-naphthol ($m/z = 144.1$ Da) is provided in Figure 7A. Fragments formed from photoionization of NDA and NHA (Figure 7B,C) are of the same mass (measured $m/z = 144.2$ Da). Because the preparative scale chromatography efficiently removed the 2-naphthol precursor from each product, this peak does not arise from contaminating starting material. Furthermore, increasing the intensity of the photoionization laser results in an increase in the fragment-to-parent ion ratio that can easily be measured from spectra such as those in Figure 3. This is consistent with a species generated photolytically.

A fragment mass of 144.2 Da is indicative of bond breakage between the oxygen of the ether linkage and the attached alkyl chain. However, simple cleavage of this bond would produce a 143 Da ion. Therefore, a hydride transfer must occur during fragmentation, a process that is known to occur in alkylbenzenes.[40,41] As shown in Figure 8A, fragmentation of the bond between the α and β carbons on an alkyl chain is facilitated by a hydride transfer from the γ carbon to the ring. The analogous process in NDA and NHA is depicted in Figure 8B. The radical cation product depicted in Figure 8B is an isomer of 2-naphthol, accounting for the mass equivalence of the peaks in Figure 7.

The most striking characteristic of the spectra in Figure 7 is the tailing of peaks to high mass that reflects a slow fragmentation time scale. This is particularly evident for NDA (Figure 7B) although some peak broadening is clearly apparent for NHA (Figure 7C). Because our experimental system is well-defined, the NDA fragmentation process can be accurately modeled. We assume that each point in a fragment ion time-of-flight profile corresponds to a specific time at which a parent ion decayed

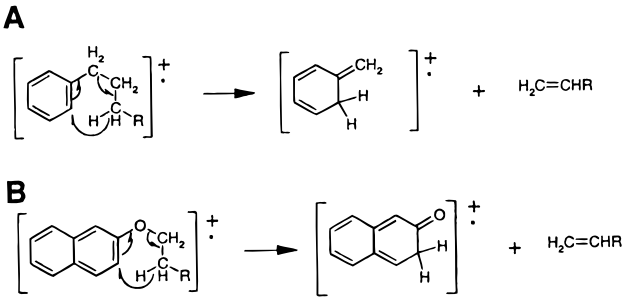

Figure 8. As elucidated by Grubb and Myerson, the radical cation of alkylbenzene fragments between the α and β carbons of the alkyl chain as facilitated by hydride transfer from the γ carbon (A).[29] Based on the mass of the fragment formed from NDA and NHA, a similar process must occur in the phototag molecules (B).

into a fragment ion in the source region of the instrument. Based on the apparatus geometry, the location of photoionization within the ion source, and the masses of the parent NDA (342.2 Da) and daughter (144.1 Da) ions, we can transform the experimental peak profile into a plot of ion yield versus daughter ion formation time. An example of data converted in this manner for generation of 144 Da daughter ions from NDA is presented in Figure 9. For simplicity, these data are expressed relative to the XeCl light pulse; ion signal at $t = 0$ ns corresponds to a 144 Da daughter ion formed instantaneously upon 308 nm irradiation of NDA. To estimate the fragmentation time constant, we fit the data with exponential functions. As displayed in Figure 9A, a single exponential (eq 3) approximately fits the data although a double exponential (eq 4, Figure 9B) provides somewhat better results:

$$y = y_0 + ae^{-bx} \tag{3}$$

$$y = y_0 + ae^{-bx} + ce^{-dx} \tag{4}$$

(The y_0 parameter has no physical significance. It simply compensates for the nonzero baseline of the original spectra which is commonly observed in experiments with MALDI ion sources).

The latter result suggests that two processes with different time constants occur during NDA photofragmentation. From analysis of several data sets, we determined that a fast decay of 13 ± 4 ns is accompanied by a slower process with a time constant of 69 ± 5 ns. Although the ionization potential of NDA has not been reported, one would expect it to be similar to that of 2-naphthol, 7.85 eV. In this case, two 308 nm photons (8.06 eV total) would ionize NDA and absorption of additional photons is likely required to initiate its fragmentation. We speculate that the slower fragmentation process arises from the introduction of a third photon into the chromophore and that the faster fragmentation occurs following absorption of a fourth photon. If this were correct, we would expect to see the relative weighting of these exponentials, given by a and c in Equation 4, to change with 308 nm light intensity. Figure 10 is a plot of our measured exponential weighting coefficients as a function of XeCl laser intensity. Consistent with the hypothesis, the extent of fast fragmentation increases and the extent of slow fragmentation decreases at higher laser intensity. (A more quantitative treatment of the observed phenomenon is not warranted because of the limited signal-to-noise ratio of the data and the ubiquitous occurrence of saturation effects in multiphoton ionization intensity dependence experiments.)

Building on this information about the photochemical propensities of NDA and NHA, we return to the subject of NDA-

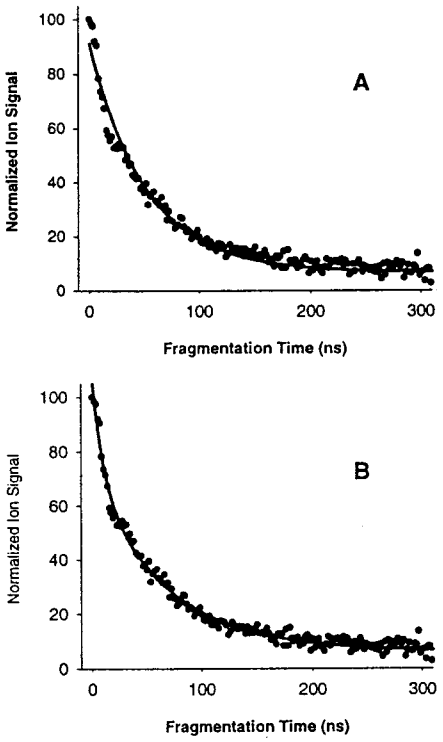

Figure 9. Deconvolution of Figure 7B data to derive NDA ion fragmentation times relative to the firing of the photoionization laser (A) single-exponential fit ($y = y_0 + ae^{-bx}$) to the data (B) double exponential fit ($y = y_0 + ae^{-bx} + ce^{-dx}$).

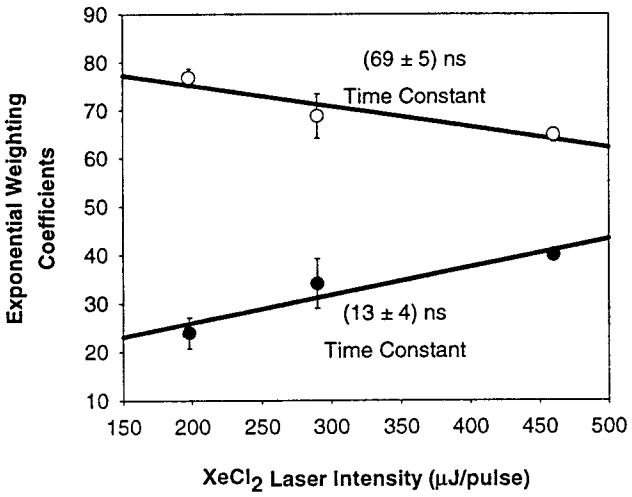

Figure 10. Dependence of exponential weighting coefficients *a* and *c* from eq 4 on photoionization laser intensity. As laser intensity increases, the contribution from the fast fragmentation process (closed circles) increases while that of the slower fragmentation process (open circles) diminishes.

and NHA-tagged bradykinin. The spectrum of NHA−bradykinin in Figure 6D contains the same 144 Da fragment ion at 6.0 μs that is produced from NDA and whose analysis was just discussed. An expanded view of this region is displayed in Figure 11. Although the signal-to-noise ratio is somewhat limited, it is evident that two peaks appear at this mass with a splitting of about 1 Da. This signal does not arise from fragmentation of residual NHA because the NHA−bradykinin was HPLC-purified; the absence of a peak at $m/z = 258.1$ Da in Figure 11 confirms the lack of NHA contamination in the sample. Control experiments run with each laser alone do not generate either component of this split peak, confirming that it is not background pump oil ionization or a low-mass MALDI

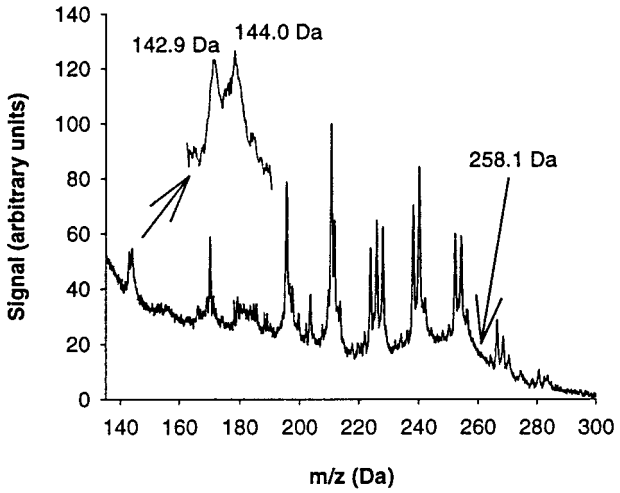

Figure 11. Photoionization mass spectrum of NHA−bradykinin expanded from Figure 6D. The inset displays the chromophore fragment ion. Note that there is no evidence for an ion at 258.1 Da that would correspond to intact NHA. Since the photoionization conditions employed here would produce NHA and its fragment in equal abundance, the fragment ion at 144 Da must originate from NHA−bradykinin.

ion. Because this signal can only be generated by the fragmentation of NHA−bradykinin, we conclude that *some NHA−bradykinin photoionizes, but after this the naphthol chromophore breaks off at the ether linkage during acceleration in the ionization source.* The fragment ion yield is quite poor; the spectrum in Figure 11 was acquired by signal-averaging 1000 individual laser shots. For comparison, the spectra in Figure 7B,C are averages of only 100 shots. An even better comparison of the relative intensities of the $m/z = 144$ Da peaks is afforded by exploiting the pump oil background ionization peaks as internal calibrants. As clearly seen in Figure 11, the $m/z = 144$ Da peak is *weaker* than the pump oil peaks that appear between about 170 and 270 Da. In contrast, this peak is much *stronger* than the pump oil signals appearing in Figure 3. Thus, we conclude that the yield of 143 and 144 Da ions obtained from NHA−bradykinin is very low indeed, again confirming that the biological molecule is not efficiently photoionizing and fragmenting.

The production of a 143 Da fragment ion must involve bond breakage of the ether linkage without the hydride transfer depicted in Figure 8. Data in Figure 7 suggest that as the alkyl chain length increases, fragmentation at the naphthol linkage is hindered and occurs on longer time scales. On this basis, we postulate that the steric bulk of the side chain hinders the approach of the γ carbon toward the naphthalene ring. In the case of NHA−bradykinin, we suspect that the peptide's considerable additional bulk further hinders the hydride transfer, sometimes causing the molecule to dissociate without rearrangement, creating the $m/z = 143$ Da ion.

Although the conditions of these experiments were quite clearly defined, two aspects were not totally controlled and require further comment. One involves the ionization state of the MALDI-desorbed molecules. It is commonly argued that there are far more neutral molecules than ions desorbed in the MALDI process. This is reasonable because the number of MALDI ions detected in an experiment is certainly far fewer than the number of sample molecules deposited in the matrix. In our experiments, we tagged amino acids and peptides at their N-termini. If blocking this basic site has any effect on ionization efficiency at all, it should be to increase the neutral-to-ion ratio in the MALDI desorption process, implying that a plethora of

neutral molecules should be available to ionize. A second complication is that we could not be certain that exactly the same quantity of each tagged molecule was introduced into the spectrometer. This prevents us from drawing quantitative conclusions about relative photoionization yields. Nevertheless, the data displayed in Figures 5 and 6 indicate that sufficient quantities of tagged biomolecules were present to produce ample ion yields through the MALDI process.

Conclusion

We conclude from these studies that the binding of a chromophore to bradykinin and a few smaller biological molecules does little to facilitate their two-photon ionization by ultraviolet laser light. Some of the photon energy imparted to the derivatized peptides is channeled into fragmentation of the chromophore label at the ether linkage. However, the fragment ion yield is very poor. Therefore, although we observe evidence that some derivatized bradykinin ionizes before it fragments, the poor yield of this process suggests that it is not efficient as suggested by Becker and Wu.[23] In fact, these experiments reveal that these molecules are quite resistant to laser-induced photoionization, despite the long alkyl chain added between chromophore and peptide in hopes of confining excitation to the chromophore. The jet cooling utilized by Frey and Holle,[22] Li and Lubman,[25] Weyssenhoff et al.,[26] and Anex et al.[28] appears to be essential for photoionizing biological molecules of even modest size.

Acknowledgment. This work has been supported by the National Science Foundation. The authors thank Stephen Antonelli (Indiana University) for his assistance with the synthesis of NHA and NDA and Ernest Davidson for helpful discussions.

References and Notes

(1) Johnson, P. M.; Berman, M. R.; Zakheim, D. *J. Chem. Phys.* **1975**, *62*, 2500.
(2) Andreyev, S. V.; Antonov, V. S.; Knyazev, I. N.; Letokhov, V. S. *Chem. Phys. Lett.* **1977**, *45*, 166.
(3) Johnson, P. M. *Acc. Chem. Res.* **1980**, *13*, 20.
(4) Meek, J. T.; Long, S. R.; Reilly, J. P. *J. Phys. Chem.* **1982**, *86*, 2809.
(5) Anderson, S. L.; Rider, D. M.; Zare, R. N. *Chem. Phys. Lett.* **1982**, *93*, 11.
(6) Kimura, K. *Adv. Chem. Phys.* **1985**, *60*, 161.
(7) Pratt, S. T.; Dehmer, P. M.; Dehmer, J. L. In *Advances in Multi-Photon Processes and Spectroscopy*; Lin, S. H., Ed.; World Scientific: Singapore, 1988; p 69.
(8) Rockwood, S.; Reilly, J. P.; Hohla, K.; Kompa, K. *Opt. Commun.* **1979**, *28*, 175.
(9) Reilly, J. P.; Kompa, K. L. *J. Chem. Phys.* **1980**, *73*, 5468.
(10) Neusser, H. J.; Boesl, U.; Weinkauf, R.; Schlag, E. W. *Int. J. Mass Spectrom. Ion Processes* **1984**, *60*, 147.
(11) Boesl, U.; Weinkauf, R.; Weickhardt, C.; Schlag, E. W. *Int. J. Mass Spectrom. Ion Processes* **1994**, *131*, 87.
(12) Schlag, E. W.; Grotemeyer, J.; Levine, R. D. *Chem. Phys. Lett.* **1992**, *190*, 521.
(13) Schlag, E. W.; Levine, R. D. *J. Phys. Chem.* **1992**, *96*, 10608.
(14) Weinkauf, R.; Aicher, P.; Wesley, G.; Grotemeyer, J.; Schlag, E. W. *J. Phys. Chem.* **1994**, *98* (8), 8381.
(15) Hillenkamp, F.; Karas, M.; Beavis, R. C.; Chait, B. T. *Anal. Chem.* **1991** *63*, 1193.
(16) Karas, M.; Bahr, U.; Giessmann, U. *Mass Spectrom. Rev.* **1991**, *10*, 335.
(17) Spengler, B.; Karas, M.; Bahr, U.; Hillenkamp, F. *Ber. Bunsen-Ges. Phys. Chem.* **1989**, *93*, 396.
(18) Wiley, W.; McLaren, I. *Rev. Sci. Instrum.* **1955**, *26*, 1150.
(19) Opsal, R.; Owens, K.; Reilly, J. P. *Anal. Chem.* **1985**, *57*, 1884.
(20) de Heer, W. A. *Rev. Mod. Phys.* **1993**, *65*, 611.
(21) Arnold, R. J.; Reilly, J. P. *J. Am. Chem. Soc.* **1998**, *120*, 1528.
(22) Frey, R.; Holle, A. *Proceedings of the 38th ASMS Conference on Mass Spectrometry and Allied Topics*, June 1990, Tucson, Arizona, p 212.
(23) Becker, C. H.; Wu, K. J. *J. Am. Soc. Mass Spectrom.* **1995**, *6*, 883.
(24) Reilly, P. T. A.; Reilly, J. P. *Rapid Commun. Mass Spectrom.* **1994**, *8*, 731.
(25) Li, L.; Lubman, D. M. *Appl. Spectrosc.* **1988**, *42*, 411.
(26) Weyssenhoff, H. V.; Selzle, H. L.; Schlag, C. W. *Z. Naturforshung Tei1 A*, **1985**, *40A*, 674.
(27) Srinivasan, J. R.; Romano, L. J.; Levis, R. J. *J. Phys. Chem.* **1995**, *99*, 13272.
(28) Anex, D. S.; de Vries, M. S.; Knebelkamp, A.; Bargon, J.; Wendt, H. R.; Hunziker, H. E. *Int. J. Mass Spectrom. Ion Processes* **1994**, *131*, 319.
(29) Rabalais, J. W. *Principles of Ultraviolet Photoelectron Spectroscopy*; John Wiley and Sons: New York, 1977.
(30) Kim, S.; Kim, Y. C.; Lee, J. I. *Tetrahedron Lett.* **1983**, *24*, 3365.
(31) Allen, C. F. H.; Gates, J. W. *Org. Synth. Coll.* **1955**, *3*, 141.
(32) Solomons, T. W. G. *Organic Chemistry*, 5th ed.; Wiley: New York, 1992; p 1114.
(33) Kowalack, J. A.; Walsh, K. A. *Protein Sci.* **1996**, *5*, 1625.
(34) *The Merck Index, 12th ed.*; Budavari, S., Ed.; 1996.
(35) Christian, N. P.; Colby, S. M.; Giver, L.; Houston, C. T.; Arnold, R. J.; Ellington, A. D.; Reilly, J. P. *Rapid Commun. Mass Spectrom.* **1995**, *9*, 1061.
(36) Berlman, I. B. *Handbook of Fluorescence Spectra of Aromatic Molecules*, 2nd ed.; Academic Press: New York, 1971.
(37) Levin, R. D.; Lias, S. G. *Ionization Potential and Appearance Potential Measurements, 1971−1981*; National Bureau of Standards: Washington, DC, 1982.
(38) Beavis, R. C.; Chait, B. T. *Chem. Phys. Lett.* **1991**, *181*, 479.
(39) Chan, T.-W. D.; Thomas, I.; Colburn, A. W.; Derrick, P. J. *Chem. Phys. Lett.* **1994**, *222*, 579.
(40) Grubb, H. M.; Meyerson, S. In *Mass Spectrometry of Organic Ions*;. McLafferty, Ed.; Academic Press: New York, 1963; p 453.
(41) Opsal, R. B.; Reilly, J. P. *Anal. Chem.* **1988**, *60*, 1060.